IPST TECHNICAL PAPER SERIES

NUMBER 352

RELATIONSHIP BETWEEN FLOW INSTABILITY IN SHORT DWELL PONDS AND

CROSS DIRECTIONAL COAT WEIGHT NONUNIFORMITIES

N.G. TRIANTAFILLOPOULOS AND C.K. AIDUN

MARCH, 1990

Relationship Between Flow Instability in Short Dwell Ponds and

Cross Directional Coat Weight Nonuniformities

N.G. Triantafillopoulos and C.K. Aidun

For presentation at the
1990 TAPPI Coating Conference, Boston, MA
May 13-16

RELATIONSHIP BETWEEN FLOW INSTABILITY
IN SHORT DWELL PONDS
AND CROSS DIRECTIONAL COAT WEIGHT NONUNIFORMITIES

N.G. Triantafillopoulos
Graduate Student

C.K. Aidun
Assistant Professor

The Institute of Paper Science and Technology
575 14th Street, N.W.
Atlanta, Georgia 30318

ABSTRACT

Short dwell coaters have received widespread acceptance, particularly for light weight coated grades, due to their operational advantages in terms of runnability and compactness. The trend toward increasing machine speed while reducing coat weight, however, has been hindered by the difficulty of attaining uniform coat weight profiles, particularly when applying formulations containing delaminated clays. It has been suggested that the three-dimensional instabilities which develop in the pond upstream of the blade may be a possible cause of nonuniform coat weight profiles. Such flows determine the transport phenomena which influence the mass and momentum transfer into the blade nip and, hence, could be indirectly responsible for film thickness nonuniformities. The main objective of the study presented in this paper is to examine this hypothesis and to establish the importance of the connection between expected flows in short dwell ponds and the "streaky" appearance of light-weight coated paper. The approach is to use flow visualization experiments with a cavity simulating a typical short dwell pond and, using pilot plant trials, to systematically document the onset and appearance of streaks. Flow visualization studies primarily used transparent Newtonian fluids and pilot plant trials used a problematic coating color with delaminated clays.

Flow visualization studies revealed multiple steady states and successive states of unstable three-dimensional flows as the characteristic Reynolds number (based on lid velocity and cavity width) increased. Centrifugal instabilities induce formation of three-dimensional patterns which drive the hydrodynamic system sequentially to time-periodic motion and eventually to more complex flows.

Within the range of shear viscosity for the high-viscosity colors investigated, appearance of streaks on light-weight coated papers correlates with expected onset of hydrodynamic instabilities in the pond. For a pilot coater having a span-to-width ratio, S = 10, streaks appear in their marginal form for a Reynolds number ranging from 550 to 750 (based on 100 rpm Brookfield viscosity and coater pond width), and in their severe form for values greater than 1100. These results, obtained with viscosity of at least 900 mPa.s, suggest that pond hydrodynamics are at least partly responsible for the streaks.

In addition, a new feature of the flow behavior was discovered in the flow visualization experiments—existence of multiple steady states with unique flow structures at the same roll speed. This proves that it is possible for a short dwell coating system to operate at different flow states with the same machine speed. This important physical property, if explored in more detail, can be controlled and used with significant advantages. Although a direct correlation between the current results from laboratory flow visualization experiments (with a cavity of span ratio S=3) and pilot coater trials (S=10) is not possible because of geometric differences, the qualitative results presented here show that, in general, the pond hydrodynamics significantly influence the coat weight profile. The potential to control the dynamics of the coating system at a given machine speed warrants an indepth and quantitative investigation of the influence of geometry on local as well as global hydrodynamic stability properties of flow in the pond upstream of the blade.

KEYWORDS

Blade Coater, Short Dwell Coater, Fluid Dynamics, Coatability, CD profile, Rheology.

INTRODUCTION

Short dwell coaters (SDC) have gained popularity over the past ten years due to their compactness, operational efficiency, and increased productivity. In contrast to systems with an applicator roll, color penetration of the sheet prior to metering is minimal and, all other parameters remaining constant, a certain coat weight can be attained with lower blade pressure. Thus, not only are paper strength properties retained, but web breaks are also reduced.

The trend toward increasing machine speed while reducing coat weight in bevelled blade operations of a short dwell coater has been hindered by difficulty in maintaining uniform cross directional (CD) coat weight profile, especially in the production of light weight coated papers for rotogravure. Spatially and temporally periodic, sometimes even random coating thicknesses create an uneven CD profile which, in its extreme case, appears as a patterned surface characterized by streaks running along the machine direction. Streaks 2-8 cm in width, also called patches, comprise areas of comparatively low film thickness which are independent of base stock formation characteristics. The macroscale streaking pattern is visually more profound when using large portions of delaminated clays—pigments desirable for their print quality but whose runnability is not conducive to high machine speeds and solids content. For example, when formulations containing more than 80% delaminated clays at solids contents above 58% or having Brookfield shear-viscosities above 1000 mPa.s (@100 rpm) are used to apply 6-10 g/m^2 coat weight at speeds above 1000 m/min. Thus, it seems there is a coatability limit in the sense that, for a given set of operating conditions and fluid viscosity, a maximum coating speed exists above which, for a slight increase in machine speed, the CD coat weight profile is uncontrollable, i.e., with variations beyond statistically acceptable levels.

Motivated to unveil a possible origin of these coat weight nonuniformities, we performed a fundamental, systematic investigation of the fluid dynamics in SDC ponds. In particular, we sought proof that three-dimensional hydrodynamic instabilities inside the pond may indirectly be responsible for, and hence correlate with, wet-film thickness variations across the machine direction. Disturbances in the pond can be transported, influencing the mass and momentum transfer into the blade nip and, consequently, affecting coat weight and uniformity. Central to this hypothesis is the thickness and uniformity (along the span of the doctoring blade) of the coating color layer traveling with the moving web which is

eventually delivered into the blade nip (Fig. 1). In systems with an applicator roll and absence of film splitting at the application nip, this layer is well-defined. A fundamental difference exists between the characteristics of the layer entering the blade nip of a SDC compared to the nearly irrotational layer [22] in a roll applicator system. In the case of a SDC, a viscous layer forms near the dynamic contact line, upstream of the blade. This layer is susceptible to instability and interaction with the dynamic contact line or the three-dimensional patterns that form when the nearly irrotational eddies inside the pond destabilize. These interactions generate a nonuniform wavy layer entering the blade nip, which could produce adverse consequences in terms of coat weight profile.

Figure 1. Schematic of the bevelled blade coating process (not in scale).

The isothermal confined flow in SDC ponds, like the flow in a lid-driven rectangular cavity, is induced by the shear stress imposed on the fluid by the moving web. Eklund, et al., using both flow visualization experiments [8] and limited numerical simulations [7] conclude that two-dimensional recirculating vortices prevail inside the pond. These authors also suggest that centrifugal forces of the two-dimensional recirculating vortices may generate viscosity stratification by inducing localized concentration gradients of pigment particles. The concentration gradients referred to by these authors, however, are in a plane parallel to the machine line direction. This alone cannot generate coat weight

nonuniformities in the CD, the topic which is of primary concern in this study. A more rigorous analysis of the apparent[*] two-dimensional steady flow state ("2D") in the pond is given by Aidun and Triantafillopoulos [3]. Although all of the computer models of SDC pond flows [1, 32, 33] consider only the two-dimensional equations and therefore cannot predict flow instability or transitions to the three-dimensional states, they provide useful information since they confirm the existence of strong recirculating eddies and reaffirm the vulnerability of the flow to three-dimensional instabilities. Thus, the question that remains is how and to what degree does the transition from the "2D" state to more complex flows influence the outcome of the coat weight nonuniformities in CD.

Although "turbulence" in the SDC pond has been proposed by many authors [4-6, 15, 25-27] as the possible cause for coat weight profile nonuniformity, there are no published experimental data or other systematically documented evidence to support this argument. Not only is it possible for various forms of hydrodynamic instabilities to set in, but the system may also have multiple stable states. Such effects can induce three-dimensional cellular structures in the pond, which eventually convect into the blade nip and may cause coat weight variations. Revealing the rich nature and forms of these flows contributes to appreciation of the differences observed in practice between systems with an applicator roll and short dwell coaters. In addition, understanding the physics involved will lead to better control of the process. Finally, information on the fluid flow aspects would provide the basis for the design of the future generation of coaters.

The methods implemented to investigate the fluid dynamics in SDC ponds is comprised of (a) laboratory flow visualization experiments in a geometry similar to a short dwell pond, and (b) pilot plant trials. As the emphasis in this paper is concentrated on experimental results, the goal is to attempt to connect what is going on inside the pond with the appearance of visible wet streaks on the coated web. Flow visualization experiments were performed primarily with a Newtonian fluid (i.e., glycerol/water) and limited studies with a coating color using aluminum-flakes, direct dye-injection, and flash x-ray radiographic techniques. This work focuses on qualitative features of the fully developed flow which

---

[*] The word "apparent" is used to signify the fact that although the flow appears to be two dimensional, in a finite span cavity, the velocity components in the third direction (CD) are small but nonzero. This can be deduced from simple fundamental characteristics of confined flows [3].

appear as the speed which drives the flow progressively increases. Pilot coater trials with coating colors were based on a typical formulation for rotogravure, which has delaminated clays and Brookfield shear-viscosity in excess of 900 mPa.s (cps).

The main body of the paper is divided into two parts. After a background description of methods and techniques used, the first part describes qualitative flow phenomena from the laboratory facility. The second part contains background information and presents the results from pilot plant trials. A separate section at the end discusses the implications of the results of this work.

LABORATORY EXPERIMENTS

Background

The flow in short dwell coater ponds has been simulated experimentally as a shear-driven flow in a rectangular cavity (Fig. 2). Futhermore, to incorporate the essence of relevant physics, a relatively small flux of fluid was allowed to pass through the cavity. Enclosed lid-driven cavities constitute a relatively simple geometry to study recirculating flows in fluid dynamics and have been used extensively, at least in their two-dimensional form, as a benchmark problem to test numerical codes. The flow is characterized by a Reynolds number (Re) defined as:

$$Re = \rho VD/\mu \tag{1}$$

where V is the velocity of the lid which induces the flow, D is the width of the cavity, and μ and r are the viscosity and density of the fluid, respectively. In this study, we consider only a depth-to-width aspect ratio of one, which is typical for short dwell coaters. For cavities with through-flow, however, an additional dimensionless parameter is required to uniquely define the flow. This is the Reynolds number (Re*) based on the net mass flow rate, m, and the span (along the CD), S:

$$Re^* = \frac{m}{\mu S}. \tag{2}$$

Flow visualization experiments performed during the course of this study were for Re between 100 and 9000, while the range for Re* varied from 0.01 to 2.40. Within this range, the through-flow cavity (Re* ~ 2.4) has flow characteristics similar to a nearly enclosed lid-driven cavity (Re*~.01).

The enclosed lid-driven cavity flow has been studied extensively both experimentally and computationally. A comprehensive review of the literature is included elsewhere [16]. Here we highlight key characteristics of the flow, as determined from previous experimental work, which has relevance to the visualization experiments performed during the course of our work.

A   Principle Direction of Flow   **B**

side-end
view

CAVITY

**Feed
Stream**

FEEDING CHAMBER

front-end view

Figure 2. Schematic of a lid-driven cavity with through-flow. (Dimensions not in scale.)

U

A   *E*

Primary
Recirculating
Roll

G   *F*

Separation between
Primary and
Secondary
Flows

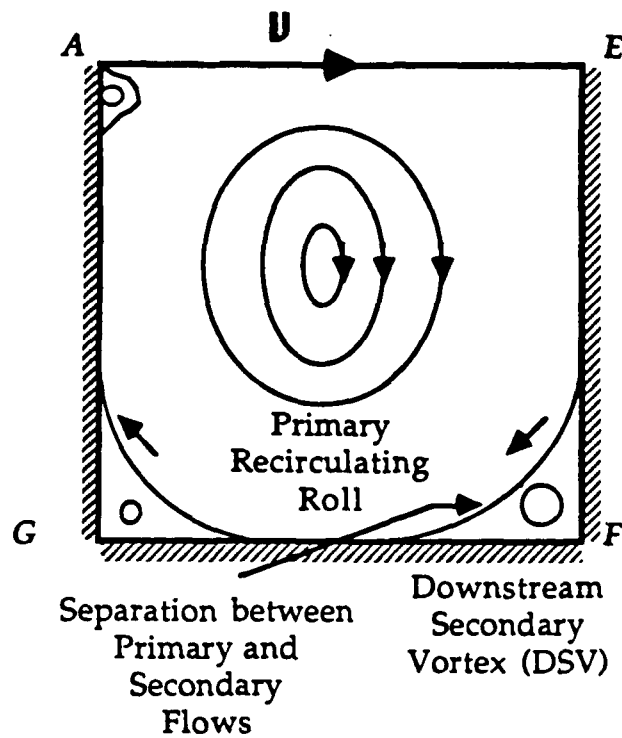Downstream
Secondary
Vortex (DSV)

Figure 3. Schematic of a lid-driven cavity with through-flow. (Dimensions not in scale.)

The two-dimensional flow depicted in Fig. 3 represents the basic stable state of the system. The primary recirculating vortex (a roll in three dimensions) drags fluid from the top lip of the cavity, E, down along the vertical downstream wall, EF. However, at some distance along the wall separation occurs and the downstream secondary vortex (DSV) forms. Similarly, secondary vortices appear at the lower and upper corners of the upstream vertical wall, AG. These flows are weaker than the primary roll but may have some impact on the flow. In general, these vortical structures have also been resolved by numerical simulations.

The most recent experimental studies of lid-driven cavities are by Kossef [16], Kossef and Street [18], and more recently by Prasad and Kossef (1989). They use an impulsively started lid to approach specific Reynolds numbers between 1000 and 10000. The three main conclusions of their work are: (a) for Re>1000, the flow is three-dimensional, exhibiting Taylor instabilities during startup and Taylor-Görtler-like (TGL) vortices when fully developed, (b) end-wall effects influence the flow by inducing three-dimensionality, and (c) turbulence occurs for Re above 6000. Most of the activities take place in the vicinity of the DSV, which led Koseff and Street [18] to suggest that these centrifugal instabilities arise from destabilization of the boundary layer between the primary and secondary rolls. It is worth emphasizing that existence of these vortices does not indicate turbulent flow, which was reported to appear only for Re between 6000 and 8000 [18]. However, the transitional mode of these evolving structures as a function of Re was not studied. Also, the rich and interesting characteristics of flow at Re<1000 where most coating systems operate has remained mostly unexplored.

EXPERIMENTAL SET-UP

In the context described above and considering actual practices in short dwell coating operations, the key to simulating the pond flow is dynamic similarity between the experimental cavities and SDC ponds. This can be achieved by matching the two dimensionless numbers Re and Re*. The geometric scales with respect to depth and width were identical with D/H =1 (H is the depth of the cavity) and physical dimension of 5.08 cm (width in the case of SDC ponds is considered the distance between the bevel of the blade and the overflow baffle). The span of the experimental cavity used is 15.24 cm and gives a span aspect ratio of 3. Admittedly, this is much smaller than the span aspect ratio

of the actual short dwell coaters (~10). So, the results from this study are mainly qualitative. The Reynolds number Re in SDC ponds can attain values from several hundreds to a few thousands depending on speed and color viscosity (e.g., Re equals 1400 for 1200 m/min (4000 fpm), machine speed, blade-to-baffle distance of 5.00 cm, r=1.40 g/cc, and μ=1000 mPa.s). The value of simple shear viscosity (called viscosity hereafter) chosen for the calculations is based on a measurement with a Brookfield viscometer at 100 rpm (spindle no. 3)—a valid quantity considering that the bulk of the fluid inside a pond experiences relatively low shear rates of the order of magnitude of a few hundred reciprocal seconds. In the case of coating colors, hence viscosity is shear- and time-dependent, only an "apparent" Reynolds number can be calculated based on this type of a single-point viscometric measurement. The Reynolds number Re* is proportional to the pumping rate which typically varies between 4 and 14 m^3/hr. The dimensionless parameters of the cavity were altered by changing first the peripheral speed of the roll, V, and second the fluid viscosity, μ, and feeding flow rate. However, the range over which fluid properties and experimental operating conditions could vary was limited by practical considerations.

The principal component of the experimental set-up is the cavity (Fig. 2) upon which a rotating cylindrical roll supplying the driving force rests. The cavity is manufactured from Plexiglas for easy visualization. The lower surface comprises the feeding chamber through which fluid enters the cavity area via a ~3 mm wide slot plate (3 mm holes, 40% open) next to the upstream vertical wall, ABKG. A 1.0 cm thick Teflon® collar around the cavity lip, ABCE, allows for smooth contact with the roll surface. A thin film is deposited onto the roll and exits the cavity from edge EC, very much like the physical arrangement in a bevelled blade SDC. Because the interest here is the flow phenomena in the cavity, no overflow was allowed for, thus excluding the influence of the moving contact line upstream. Air inclusion in the cavity may occur as the roll speed increases, but it can be avoided by properly adjusting the feeding flow rate and the hydraulic pressure that keeps the cavity in contact with the roll. More details on the experimental facility and its operation are included elsewhere [30].

In most of the flow visualization experiments, we used various mixtures of glycerine in water having viscosity between 77 and 160 ± 3 mPa.s (Brookfield viscometer, spindle no. 3, 100 rpm) and density of 1.26 to 1.28 ± 0.04 g/cc. A limited number of visualization experiments were conducted with a sodium alginate solution (μ=95 mPa.s and r=1.1 g/cc).

The preferred method for visualization was the suspended-particles technique [23] where disk-shaped, high reflectance aluminum flakes (340 mesh) are suspended in the fluid continuum at concentrations of up to 0.1% by weight. These flakes act as neutrally buoyant markers which, on videotape, show photographic images of the instantaneous state of flow, or the evolution of periodic and unsteady states. In addition, direct-dye injection techniques [20] were also used to indirectly reveal the accumulated results of transport processes occurring in the cavity. This technique can unveil the form of flow structures. Some qualitative data were obtained with typical coating colors at 60% solids content by using the newly developed flash x-ray radiographic (FXR) technique described in a previous paper [31]. The tracer here was a CMC solution containing approximately 50% by weight sodium tungstate, a substance which has one of the highest mass x-ray absorption coefficients. The density and viscosity of this fluid were similar to the coating color.

FLOW VISUALIZATION RESULTS

We evaluated phenomena appearing in driven cavity flows with through-flow using real-time observation and photographs of flow patterns in a laboratory facility. The flow in the cavity is changed by increasing the roll speed in increments. The photographs presented here depict the front view of a cavity as a spanwise plane parallel to downstream wall EFCN in Fig. 2. Limited observations from a side-end view parallel to end-wall AEFG reveal the basic flow characteristics illustrated in Fig. 3, thus confirming the similarity of the flow considered here and the enclosed lid-driven flow. However, our interest is concentrated on the three-dimensional flow structures along the spanwise direction of the cavity (the CD of the machine).

The control parameter that describes the flow is the cavity Reynolds number, Re, as estimated from repeated visual observations. Gradual increase of the roll speed takes the system from its "2D" steady state (the base stable state) to time-periodic and unsteady states featuring three-dimensional cellular structures. Toroidal eddies in the form of Taylor-Görtler-like vortices meander along the spanwise direction of the cavity with their axes parallel to the principal direction of flow. These structures are consequences of centrifugal instabilities and are relatively weak flows at onset but grow in strength with roll speed. Similar structures are obtained during sudden start-up of the flow when the value of Re is above a certain critical range. Table 1 presents a rough estimate of the critical ranges and corresponding observations from flow visualization experiments using square cavities with a spanwise aspect ratio of 3. The maximum experimental error in obtaining Re is ±40, while the uncertainty in estimating the critical Re, by observing the flow with a naked eye, is about 20 percent. Therefore the accumulative error is about 30 percent. Following is a brief description of the flow patterns observed with the aluminum-flake technique.

When the cavity Reynolds number remains below approximately 500, the "2D" state is stable and steady, featuring mainly the primary and downstream secondary rolls. A front view of the two rolls appears in Fig. 4 (the dark line is the interface separating the rolls). For Re in the range of 500 to 600, vertical dark spikes are generated at the centerline and start traveling toward both end-walls (edges). At Re up to about 1100, the separation line becomes wavy and the waves subsequently oscillate in a complex spanwise direction. At this point, spikes grow small crowns which give them a mushroom-like form. As the
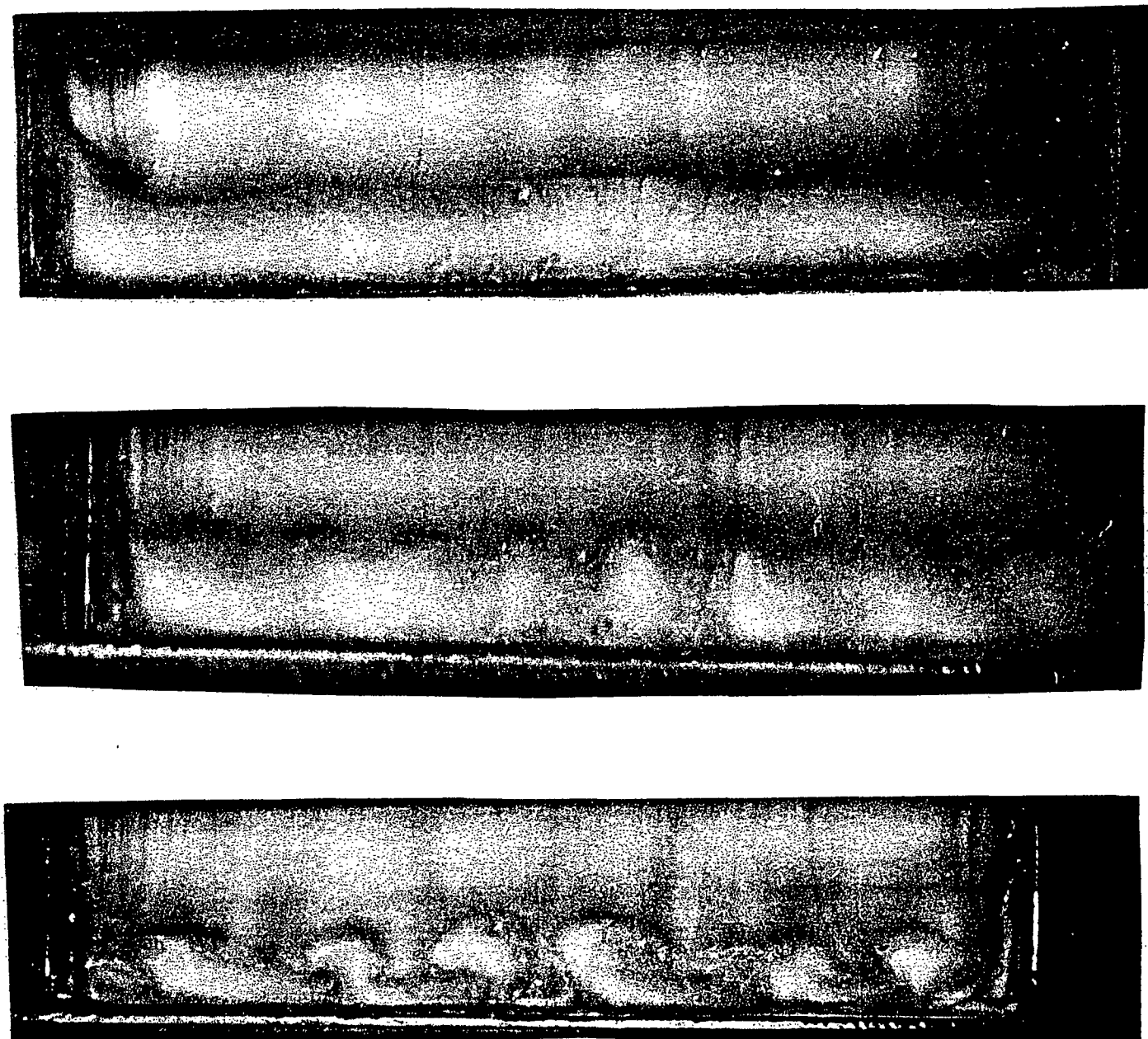
Figure 4. Front-view photographs of flow patterns: (a) two-dimensional flow with primary and downstream secondary rolls for Re<500 (notice straight separation line); (b) wavy separation line for Re=700-1000; (c) mushroom-like structures for Re>1100.

speed slowly increases, the flank and stem of the mushrooms first oscillate in-phase and eventually fluctuate causing the flanks to alternatively jump from left to right rapidly, thus giving the appearance they are disappearing into their neighbors and reappearing a short while later. This could very well be the onset of an unsteady nonperiodic state.

The direct-dye technique gives a better assessment of the kind of structures that superimpose on the base stable state because it represents accumulated results of all transport processes that carry the injected fluid. When the tracing fluid is injected close to edge EC along the (primary roll) flow down the wall EFCN (in Fig. 2) a horseshoe-shaped structure is formed inside the DSV and next to the bottom boundary (Fig. 5). These are very similar to the three-dimensional vortices arising from centrifugal instabilities in enclosed lid-driven cavity flows termed TGL vortices by Koseff [16], and Koseff and Street [17, 18]. These vortices appear in pairs along the span of the cavity, so that a horseshoe-shaped structure is riding on a pair of TGL vortices. This feature is illustrated in the shadowgraph obtained with the FXR technique (Fig. 6), where the bulk fluid is a typical coating color. Such similarities between Newtonian and coating fluids imply that flow features, prevailing above a critical range of the control parameter, exist irrespective of the type of fluid. Thus, the spikes appearing with the aluminum-flake technique represent the cross-section of the vertical interface between two neighboring TGL vortices.

Table 1. Estimated critical Reynolds numbers from flow visualization experiments. (Lid-driven cavity with small through-flow, Re* < 2.0, D=1:1, S=3:1.)

Re ($\pm 30\%$ uncertainty)	Observations
above 500	A time-periodic, three-dimensional instability superimposes on the DSV of the base two-dimensional state.
600-700	Separation line between main roll and DSV becomes wavy; waves travelling in spanwise direction from centerline.
900-1000	Violent spanwise oscillation of waves.
1100 and up	Unsteady mushroom-like forms fluctuate violently inside the DSV.

The qualitative results presented above demonstrate that, as the roll speed increases, the flow in the pond of SDCs is also susceptible to centrifugal instabilities. These instabilities arise from imbalances induced by competing centrifugal forces (due to curvilinear streamlines of recirculating rolls) and the pressure gradient, created in a manner similar to the Taylor vortices appearing in circular Couette flows and the Görtler vortices appearing in boundary layer flows over concave walls. Interestingly, the sequence of evolving structures described above is similar to the sequence of events observed during the instability of a laminar boundary layer flowing over a concave wall [21].

A more intriguing and potentially useful feature of flow in the pond is the appearance of large scale three-dimensional structures at low to moderate Reynolds numbers which compete with the stable "2D" state. Depending on the procedure followed to attain a certain speed, an array of counter-rotating cellular structures stabilizes and replaces the base state. Three possible patterns are presented in Fig. 7. This is an important piece of information regarding the behavior of this hydrodynamic system. Although the multiple states of flow are stable to infinitesimal disturbances, they are unstable to finite-amplitude disturbances, i.e., the system is locally stable but globally unstable (see Aidun, 1990 for a definition). Physical characteristics, possible mechanisms for control and potential uses for multiple operating states in short dwell coaters are discussed elsewhere [3].

Three-dimensional cellular structures may have two effects. First, they unevenly distribute the fluid mass and momentum transfer into the converging nip under the blade as there are alternative regions of slow and fast moving fluid elements between the cells along the spanwise direction. Second, centrifugal forces associated with recirculating patterns can induce localized variations of the solid particles concentration, thus introducing viscosity and density stratifications. Appearance of the qualitatively similar structures with both Newtonian and shear-thinning (e.g., coating colors) fluids is not a sufficient indication that the flow characteristics can be explained by only one control parameter—the cavity Reynolds number. Instead, the flow is really a multiparameter system with more complex dynamics. A qualitative comparison could be useful to the extent that a viscosity value can be selected to represent the time- and shear-dependent rheology of coating colors. Finally, the global instability of the flow suggests the existence of multiple operational states and a possible reason for the unpredictable runnability of short dwell coaters in practice. Depending on which state the system is attracted to, identical operational conditions may or may not give trouble-free production, a potentially useful feature which needs to be explored further.

Figure 5. A direct dye-injection image of a horseshoe-shaped structure appearing in the vicinity of the downstream secondary roll near the middle of the cavity. Re=500.

Figure 6. Flash x-ray radiographic image of a pair of Taylor-Gortler-like vortices appearing in the vicinity of the downstream secondary roll near the middle of the cavity. Re=590, Re*=0.35. (Image magnified to show details.)

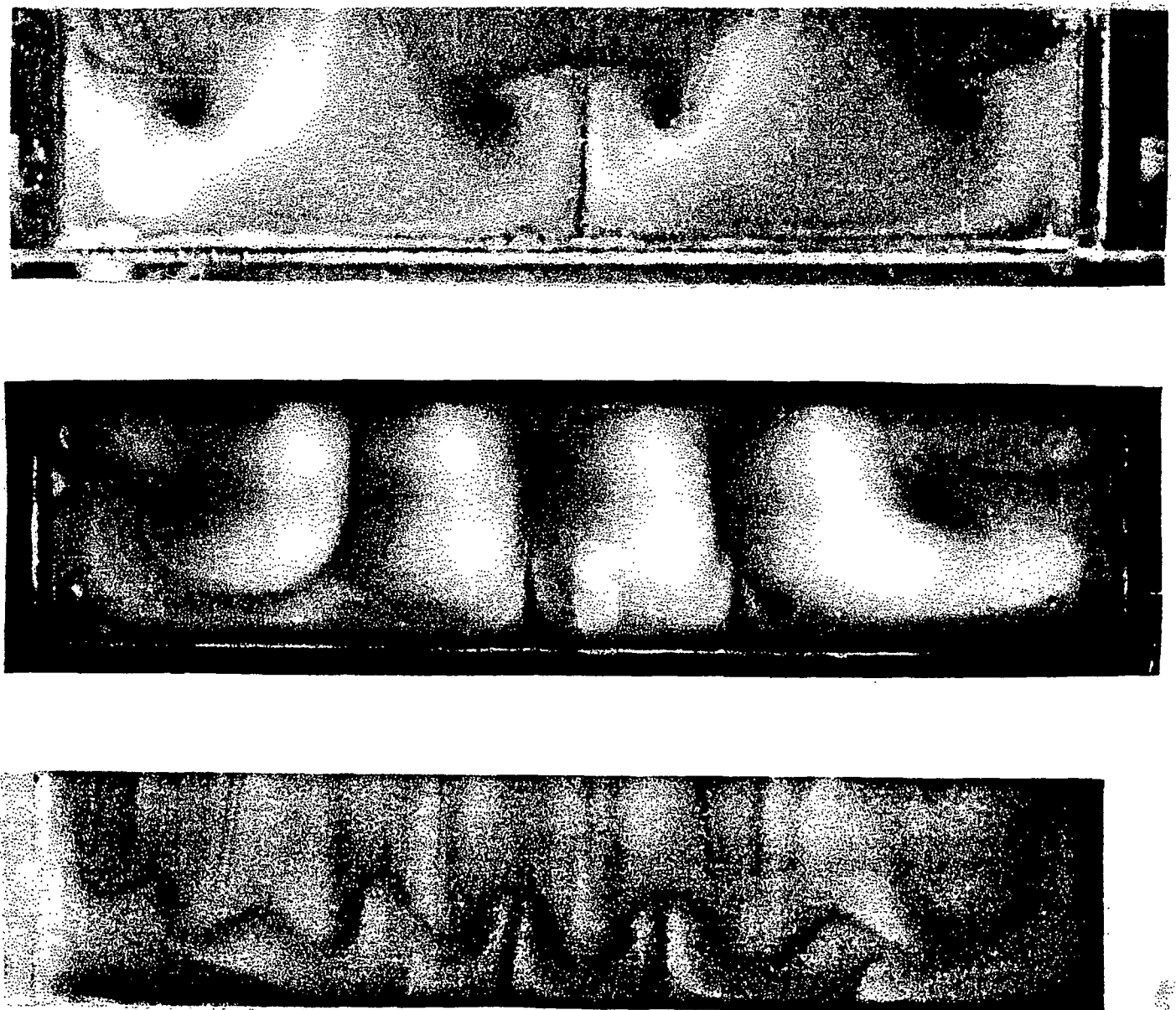**Figure 7.** Front-view of stable three-dimensional flow patterns appearing when Re<300. Re*=0.01-0.8.

PILOT COATER TRIALS

Background

Since no systematic pilot plant data have been published with respect to the occurrence of wet streaks, the task was to collect evidence that could connect visually observed wet streaks on LWC paper with expected transitions of the pond flow. Qualitative information was obtained by inspecting the coated paper with the naked eye. The hydrostatic pressure profile (along the machine direction) normal to the roll was also measured to compile quantitative data which indirectly relate to hydrodynamic phenomena in the pond.

Pilot plant trials were based on actual production practices, the only difference being the effective span of the coater, which was only 40 cm (i.e., D/H =1 , S/D = 10). In all trial runs, operating conditions were adjusted to control coat weight, while the temperature of both the sheet and the color were maintained at about 27°C. Two series of trials were performed under well-controlled conditions using a 60-g/m^2 base stock for LWC in the first series of trials and a 50-g/m^2 stock in the second series. An outstanding difference between the two series was the type of delaminated clay used in otherwise similar formulations, i.e., typical of papers printed with rotogravure. English China and Georgia delaminated clays were used in the first and second series, respectively. In general, because coating colors are non-Newtonian fluids, it is difficult to determine with confidence the effective value of the Reynolds number in complex flow fields, such as the one inside the pond. To be consistent with the flow visualization experiments, we arbitrarily chose to base the Reynolds number on the Brookfield (100 rpm) viscosity, m_B. Therefore, the parameter which defines the flow in the pond is given by an "apparent" Reynolds number Re_a as:

$$Re_a = \frac{\rho VD}{\mu_B} ,$$

(3)

where, V is the machine speed, and D, the characteristic length, is the distance between the blade tip and the baffle. The value of m_B was controlled by maintaining high solids levels (56-59%) to keep it from falling below approximately 900-1000 mPa.s which, from previous experience, has resulted in visible streaks.

It is worth noting certain rheological properties of the coating colors under consideration before presenting results from trials. In particular, our efforts concentrated on formulations

containing pigments with relatively high aspect ratio particles, i. e., above 15:1, such as
English delaminated grades which are comprised of particles platier than those in domestic
delaminated grades of clay [35]. In addition to 100 percent delaminated clay, the
rotogravure formulation contained 3.0-4.5 pph SBR latex and 0.3 pph alkali-swellable
thickener; its total solids content was approximately 58% by weight based on dry pigment.
Figure 8 demonstrates the relationship between viscosity and shear rate for ten decades of
shear using three different viscometers. The data of the formulation described above are
compared visually to a reference color, i.e., containing a domestic grade of delaminated
clay at 61% solids, that had no runnability problems for machine speeds up to 1200 m/min
(4000 fpm). Hercules® measurements were taken with the instrument on its 'SET RPM'
mode to avoid temperature buildup during a test. The scattering of this data is due to the
fact that all three bobs (i.e., A, E, and F) have been used. Brookfield data represent
measurements at four different rotational speeds of the no. 3 spindle and calculation of the
corresponding shear rates based on the procedure by Hyman [13]. The Carimed®
instrument was a controlled stress rheometer (cone-and-plate geometry) with a logarithmic
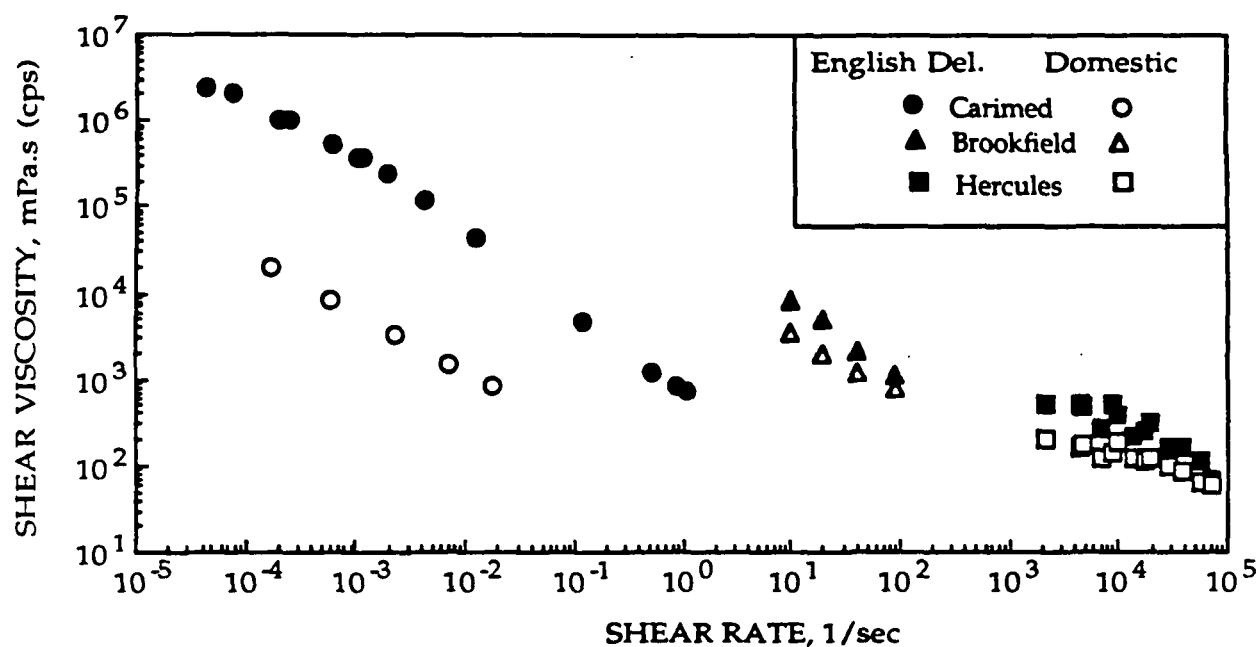stress mode. Uncertainty in the measurements with all instruments was about 10 percent.

Figure 8. Rheological data of a typical color used in pilot plant trials and of the reference color. The
first contains English delaminated clay, the second a domestic delaminated grade. Thermostatic temperature
of Carimed and Brookfield data was 25°C, of Hercules data was 20°C.

The coating color of interest is shear thinning over the range of shear rates from 10^{-5} to 10^5 sec^{-1}. Stress rheometer data illustrate that shear viscosity decreases by several orders of magnitude over the shear rate range of 0.0001 and 10 sec^{-1}. Comparatively, the reference color shows a similar trend but with viscosity values at least two orders of magnitude lower. This difference decreases substantially with increasing shear rates, as depicted from Brookfield and Hercules data in the shear rate range of 10 to 10^5 sec^{-1}. Data sets from all three instruments do not fall into a single line because of differences in the measuring geometry between the viscometers. Linear regression of the combined Brookfield and Hercules data provide the following relationship for the power-law fluid model:

$$\mu = 1.04 \, \gamma^{0.56}$$

(4)

hence constant 1.04 represents the so-termed zero-shear-rate viscosity limit μ_0 of the color, and 0.56 is the flow index N (the regression coefficient is 0.90). The value of μ_0, equal to 1040 mPa.s, is numerically similar to μ_B, so the apparent Reynolds number is roughly based on the zero-shear-rate viscosity of the color. Thus Re_a can be conveniently calculated from measurements with two viscometers commonly used in practice. Constants μ_0 and N for the reference color is 0.91 and 0.35, respectively. Interestingly, an outstanding difference between the reference color and the one of interest here is in the flow index of the power-law fluid model. In addition to the high viscosity values observed with the stress rheometer, the "problematic" color has comparatively high flow index. However, the value of its flow index does not indicate shear-thickening, which is signified for N greater than one.

RESULTS

Table 2 presents an overview of the results from the pilot plant trials. These results should be analyzed and interpreted with some caution. At first, it appears that the Pond Reynolds number, Re_a, is the only control parameter. This is not the case as we explain in the next section. The following paragraphs in this section report only the results of the pilot trials.

In both series of trials, the first occurrence of streaks appears for Re_a in the range between 550 and 750. After processing, the marginal case here shows at least one streak upon visual inspection of the web (Fig. 9). Such streaks are discontinuous narrow patches of 1-3 cm in width which run along the machine direction in an intermittent and periodic manner, which is referred to in Table 2 as *marginal* appearance of wet streaks.

As the machine speed increases and the Re_a is raised, streaks grow both in width and frequency to eventually form almost continuous bands running along the machine direction for Re_a between 800 and 1000 (Fig. 9). In their severe form, low coat weight bands cover the full CD span of the web and become visible right after the blade during high speed operations. The width of individual bands varies between 3 to 8 cm, the widest of which appears with the formulation containing the platier clay particles (English China clay). About five to six bands are counted on a 40-cm wide web coated on the pilot SDC. At even higher speeds, the bands oscillate spatially along the CD. As speed is increased further, eventually air entrainment starts from the dynamic contact line upstream of the blade. These nonuniformities cannot be corrected by adjusting the blade pressure (i.e., with the profile screws) across the machine line direction.
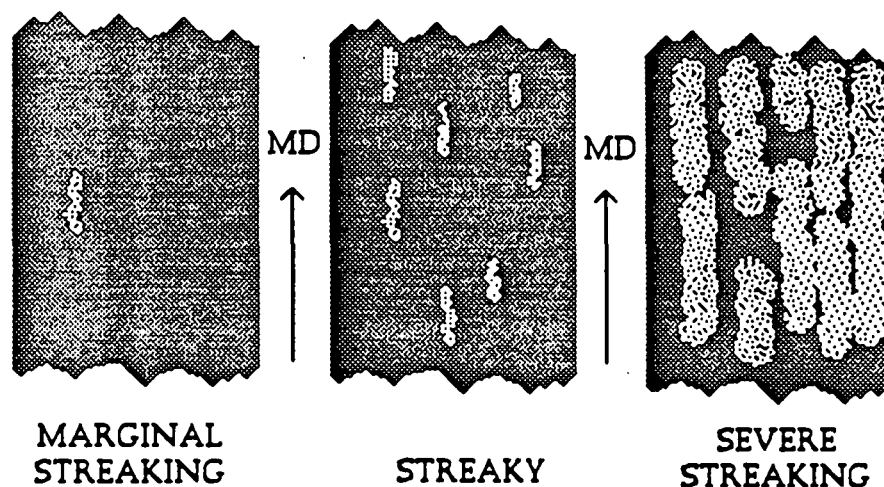

MD

MD

MARGINAL
STREAKING

STREAKY

SEVERE
STREAKING

Figure 9. Schematic illustration of the appearance of wet streaks on LWC paper during pilot plant trials.

Table 2. Visual observations from LXC papers coated in a pilot short dwell coater (45° x 0.5 x 76 mm bevelled blade, 19 mm stick-out, 3 mm baffle gap, pond D=1:1, S=10:1).[a]

Trial Run No.	Color Viscosity[b] (mPa.s)	Machine Speed (m/min)	Reynolds Number Re_a	Appearance of Wet Streaks
First Series (11gsm, pump rate 166 L/min/m)				
1	1884	305	210	No
2	1428	760	690	Yes
3	1428	800	710	Yes
4	1428	820	740	Yes
5	1428	730	660	Yes; marginal
6	1412	610	560	No
7	980	640	840	Yes
8	980	670	880	Yes
9	980	700	920	Yes
10	1236	610	635	Yes; marginal
11	1236	700	730	Yes
12	1236	490	510	No
13	1236	550	570	Yes; marginal
14	1056	610	740	Yes
15	1056	1060	1300	Yes; severe
Second Series (6-7gsm, pump rate 166L/min/mc)				
1	1268	700	790	Yes; sporadic
2c	1292	305	670	Yes; marginal
3	1268	760	850	Yes
4	1280	790	910	Yes
5	1292	820	1000	Yes
6	1224	730	1240	Yes
7c	904	305	480	No
8	1012	640	860	Yes
9	1052	1220	1650	Yes; severe
10c	1004	1340	1900	Yes; severe
11c	1104	370	470	No
12c	1120	430	540	No
13c	1156	490	600	Yes; marginal
14c	1160	550	670	Yes; sporadic
15c	1156	610	750	Yes

[a] The colors used had Brookfield viscosity of at least 900 mPa.s. Streaks do not appear at these Re values with formulations having lower viscosity.

[b] Brookfield viscosity, 100 rpm, no 3 spindle.

[c] In this case the pumping flow rate was 200 L/min/m.

The above results suggest a connection between the appearance of streaks on the coated web and the Reynolds number, Re_a, for the range over which fluid viscosity and machine speed are varied. Generally, the Reynolds number decreases with reduced machine speed, but increases with lower fluid viscosity (from Eq. 1). Good examples of this are trials 6, 10, and 14 in the first series where constant machine speed at 610 m/min (2000 fpm) may or may not produce streaks depending on viscosity and the value of Re_a. This is also true irrespective of the type of clay pigment used, i.e., trial 15 in the second series. In the same manner, increasing machine speed while maintaining constant viscosity induces streaking, i.e., trials 2 to 6 in the first series. The results show that, independent of how a certain value of Re_a is attained, streaks will appear if its value exceeds a critical number, such as in trials 2 and 14 in the second series where $Re_a=670$ represents the marginal case for appearance of streaks.

The range of Re_a over which streaks definitely occur for the first time, i.e., 550-750, is in the same order of magnitude where the initial laminar transitions from steady state to time-periodic and more complex states occur in the driven cavity flow visualization experiments (Table 1). Direct and quantitative comparisons between the two studies are only possible when the effects of geometry (i.e., spanwise aspect ratio) and fluid rheology are considered in future studies.

As the Reynolds number Re_a rises above 1000-1100, streaks fill the whole CD width and are visible to the naked eye even at production speeds. This range of Re_a is also comparable to the critical value of Re for which spanwise oscillation of the flow is observed in the experimental cavity.

Hydrostatic pressure measurements with a transducer mounted on the middle of the backing roll indirectly indicate existence of recirculating flows in SDC ponds. Figure 10 presents a typical profile with pressure values obtained for a wide range of color viscosities and operating conditions. Blade pressures are estimated from the literature [26] because their range exceeds the useful range of the transducer. Measurements under conditions of practical interest show that pressure rises to 1-9 kPa (0.2-1.3 psig) right at the baffle, with greater values corresponding to narrower baffle gaps. Inside the pond and closer to the

blade, a pressure drop occurs which may cause the pressure to become subatmospheric, e.g., -2 to 4 kPa (-0.3 to 0.6 psig). To obtain a correlation between the pressure profile inside the pond and the onset of streaks, it is necessary to measure spanwise pressure variations of the viscous layer which forms at the roll.
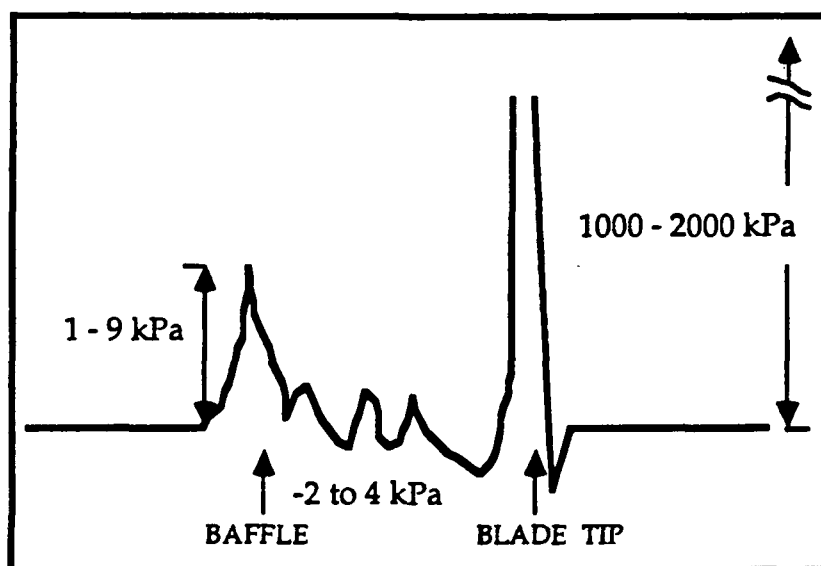

Figure 10. Hydrostatic pressure profile normal to backing roll surface in a SDC.

DISCUSSION AND IMPLICATIONS OF RESULTS

Operational differences between bevelled blade coating systems with an applicator roll and the short dwell coater cannot only be explained by the low pressure and short contact time (between the color and the web) of the latter. The fluid dynamics upstream of the blade nip are qualitatively different between the two systems. In the case of a short dwell coater, hydrodynamic phenomena in the pond can influence the local variation of color mass transport into the blade nip and the uniformity of the momentum transfer across the machine direction. Such phenomena may not only determine the spatial and temporal uniformity of coat weight, but they can also affect orientation of inherently asymmetric pigment particles, thus explaining differences in the properties of the final coated sheet.

The laminar flow in short dwell ponds is characterized by recirculating flows wherein strong centrifugal forces arise from curvilinear streamlines. The base state of flow consists of primary and secondary rolls driven by the web, its tail-end sometimes described as a "rolling sausage" over the baffle stretching along the CD of the machine. Additional weaker (secondary) rolls appear at the corners of the pond depending on the specific geometry. This state of flow comprises the ideal case from the runnability standpoint, since there is a nearly uniform stable mass of fluid delivered into the blade nip across the machine direction. However, this is not a uniquely defined state because it competes with other steady states, three of which have been identified experimentally to date. This indicates the sensitivity of the system to hydrodynamic forces. Alternative states of flow feature three-dimensional structures which are stable to infinitesimal disturbances and which, once established, do not switch to the base steady state. Such behavior provides a possible explanation for the difficulty in predicting runnability in coating operations, and for the phenomenological differences between identical coaters. By analytically determining the regions of attraction for each type of flow, it will be possible to set guidelines for desired operating states, useful information for production purposes.

As the fluid velocity increases, centrifugal instabilities in the pond generate three-dimensional evolving structures termed Taylor-Görtler-type vortices. These instabilities arise from the imbalance between centrifugal forces and pressure gradients, either inside a recirculating roll or on the layer formed at the interface between faster- and slower-moving flows, such as those between vortices. Thus, the source of such inherent fluid dynamic instabilities is internal to the system behavior. With axes parallel to the direction of web

movement, counter-rotating vortices form regions of ingoing and outgoing fluid across the blade nip which could indirectly cause uneven CD profile. Following a series of transitional modes, the pond flow eventually reaches complex unsteady states. It should be emphasized, incidentally, that appearance of cellular structures in the pond does not signify onset of turbulence.

Under the conditions investigated, observation of low coat weight streaks running along the machine line direction relates to onset of flow instabilities in the pond of a short dwell coater. In particular, appearance of severe streaking occurs when violent flow fluctuations set in along the span (cross machine direction) of the pond. When a UV dye is mixed with the coating color, small variations in UV reflectance (which is directly proportional to variations of coat weight) are enough to result in a streaked see-through appearance on LWC papers coated with 6-11 g/m^2 on one side [19]. This shows the high sensitivity of the human eye and is indicative of the difficultly in qualifying differences estimated visually. It should be pointed out, however, that the reported results correspond to coating formulations with relatively high viscosity, i.e., approximately above 1000 mPa.s as measured with a Brookfield viscometer (@100 rpm).

Practical experience has shown that if viscosity is low enough (e.g., reduced solids content or smaller pigment particles) the runnability window of short dwell coating expands to greater machine speeds. This indicates that the non-Newtonian behavior of the coating color and other factors influence the stability properties.

To elucidate these effects, several scenarios can be proposed. Let us consider one here. Because of the recirculating flows in the pond, fluid elements and other components of coating colors that are only a few millimeters away from the web move opposite to the machine direction. Only after these particles have penetrated the viscous layer that forms on the moving web when the color contacts it upstream, do they experience the viscous drag of the substrate, at which point they are accelerated and convected downstream. In systems with an applicator roll, the outer layer of the flow which deflects down the blade is irrotational [22]. In contrast, the flow in short dwell coaters contains recirculating eddies which as demonstrated above becomes unstable due to centrifugal forces and gives rise to time-periodic and three-dimensional flow patterns. Various mechanisms are available for predicting and analyzing these instabilities [2]. Cellular structures in the pond cause nonuniform orientation of pigment particles and, if there is not enough time for the particles

to reorient, the structures can create unstable conditions in the nip. As pointed out by Gane and Coggon [9], orientation phenomena of clay particles upstream of the blade can also affect the final coating properties. Such effects are generally more pronounced in formulations containing highly asymmetric particles, e.g., delaminated clays, at relatively high solids content. They may not, however, be important when using pigments with small particle size, e.g., a no. 2 grade of clay. Thus, CD profile variations can be attributed to both the hydrodynamics in the pond coupled with color properties which are proportional to viscosity. This scenario explains why below a certain solid concentration the streaks disappear, and it also explains the appearance of streaks with larger aspect ratio solids. Proof for this and other scenarios does not yet exist.

The dynamics of flow at the blade are also important and should be considered. For example, based on analysis by Higgins [12] and Guzy and Higgins [11], a positive pressure drop puts an upper limit on the final film thickness or coat weight that can be attained. Furthermore, they show that, according to lubrication theory, below a certain film thickness the steady state flow ceases to exist when the pressure gradient across the blade is positive.

As the trend in the industry shifts toward higher machine speeds and lower coat weights, film thickness imperfections put an upper limit on machine speed. This is especially important when using large, highly orientable pigment particles which give better print quality but their application is not conducive to high solids content. Results from experimental studies presented here provide important information and insight regarding the dynamics of the flow in SDC ponds. The origin of CD profile unevenness, however, remains unclear. Although a scenario has been stated for these coat weight nonuniformities, we will spare the reader from additional hypotheses until more concrete evidence can be produced, since further studies are required to pinpoint the physical origin of nonuniformities with some degree of rigor and confidence.

CONCLUSIONS

Flow visualization in a lid-driven rectangular cavity with through-flow, which experimentally simulates the short dwell pond, reveals previously unknown aspects of such flows. These are:

(1) The "2D" state, the ideal flow patterns for coating, competes with multiple steady states having three-dimensional flow patterns. Three competing states have been identified to date. The nonunique nature of steady flows can possibly be the cause of difficulty in predicting runnability in many practical situations.

(2) When the Reynolds number (the control parameter of the flow based on cavity width and viscosity) increases, centrifugal instabilities in the form of Taylor-Görtler-like vortices (vortex pairs with their axes parallel to the machine direction) prevail. They meander along the span of the cavity, progressively oscillating, and eventually evolve into more complex states. There is little doubt that similar structures also appear in the pond of short dwell coaters. Regions between these vortices are characterized by differential mass transport and uneven momentum transfer into the blade nip. Critical values of the control parameter for onset of the various transitional modes of flow have been roughly identified for cavities with a span-to-width aspect ratio of 3 to 1.

Pilot trials with SDCs and coating colors with large solid concentrations show the following features:

(1) Within the range over which the fluid viscosity was varied, appearance of streaks on LWC papers correlates with expected onset of hydrodynamic instabilities in the pond. For a pilot coater having a span-to-width ratio of 10 to 1, streaks appear in their marginal form at $550 < Re_a < 750$ and in their severe form at $Re_a > 1100$. These results indicate that pond hydrodynamics is an important factor affecting runnability of high-speed SDCs. However, they are based on viscosity values of at least 900 mPa.s attained, for example, when processing formulations containing large proportions of delaminated clays at high solids content. For lower viscosities, the streaks actually disappear, although the Reynolds number will be higher.

As stated before, the results from this study do not provide enough information to completely pinpoint the origin of streaks and to explain the physics involved. This study

has, however, increased the understanding of this problem and has proved, with concrete evidence, the existence of some new flow instability issues which may exist in short dwell coaters as well as in other coating and sizing systems with similar hydrodynamic characteristics.

Although our focus here is on problems associated with streaks in SDCs, we have established and identified several possibilities for the origin of this, and more generally, the nonuniformities occurring at high speed surface applications, some of which are discussed in this and other papers [2,3]. To pinpoint these problems, however, requires (a) systematic pilot coater trials to better document and classify these nonuniformities; and (b) a more fundamental and complete understanding of shear driven cavity flows of Newtonian as well as shear-thinning fluids, which are a subclass of SDCs, puddle coaters, and other surface application systems with recirculating eddies.

ACKNOWLEDGEMENTS

LITERATURE CITED

1. Affes, H., Conlisk, A.T., and Foster, M.R., "The Flows in a Short Dwell Coater," *Bulletin of the American Physical Society*, **34**, No. 10, 1989.

2. Aidun, C.K., "Principles of Hydrodynamic Instability in Coating Systems," Coating Conference Proceedings, TAPPI Press, Atlanta, GA, 1990.

3. Aidun, C.K., and , Triantafillopoulos, N.G., "Global Stability of Flow Structures in the Pond of a Short Dwell Blade Coater, " International Symposium on Mechanics of Thin Film Coating, *National AIChE Meeting*, March 18-22, 1990.

4. Baumeister, M., "European Coating Technology," *Pulp Paper Can.* **90**, 3, 1989.

5. Baumeister, M., "Experiences with Short-Dwell Coating Aggregates," *Coating* **19**, 11, 384-387, 1986.

6. Beisswanger, R., "Coating Paper and Board, Practical Experience with the Short-dwell and Long-dwell Time Applicators," Blade Coating Seminar Notes. TAPPI Press, Atlanta, GA, 1986.

7. Eklund, D. E., Norrdahl, P. C., "The Flow Characteristics in a Short Dwell Coater," Coating Conference Proceedings. TAPPI Press, Atlanta, GA, 1986.

8. Eklund, D.E., Strömberg, M., "Das Strömungsbild beim Short-Dwell-Blade-Strichauftrag," *Wochbl. Papierfabr.* **114**, 6, 1986.

9. Gane, P.A.C., Coggon, L., "Coating Blade Geometry: Its Effect on Coating Color Dynamics and Coated Sheet Properties," *Tappi* :87-96, 1987.

10. Görtler, H., Nachr. Akad. Wiss. Göttingen, Math. Phys. Kl. 2 (1940); translated as "On the Three-dimensional Instabilities of Laminar Boundary Layers on Concave Walls," Tech. Memorandum 1375, NACA, 1954.

11. Guzy, C. J., and Higgins, B. G., "Viscous Pressure Across the Nip of a Blade Coater and its Effect on the Final Coated Film Thickness," Coating Conference Proceedings, TAPPI Press, Atlanta, GA. 1982.

12. Higgins, B. G., "Dynamics of Coating, Adhesion and Wetting," Status Report 3328, The Institute of Paper Science and Technology (former Institute of Paper Chemistry), October 20, 1981.

13. Hyman, W. A., "Rheology of Power Law Fluids," *I & EC Fund.* **15**, 1976.

14. Kahila, S. J., and Eklund, D. E., "Factors Influencing the Coat Weight in Blade Coating with Bevelled Blades: Theory and Practice," Coating Conference Proceedings. TAPPI Press, Atlanta, GA,1978.

15. Korpela, M., Palsanen, J., and Pitkanen, S., "Practical Experience with SDTA," *Wochbl. Papierfabr.* **114**, 8, 1986.

16. Koseff, J. R., "Momentum Transfer in a Complex Recirculating Flow," Ph.D. Thesis, Department of Civil Engineering, Stanford University, CA, 1983.

17. Koseff, J.R., and Street, R.L., "Visualization Studies of Shear Driven Three-Dimensional Recirculating Flow," Proc. Three-dimensional Turbulent Shear Flows Conf., ASME, St. Louis, June 7-11, 1982.

18. Koseff, J.R., and Street, R.L., "Visualization Studies of a Shear Driven Three-dimensional Recirculating Flow," *J. Fluid Eng.* **106**, 3, 1984.

19. Li, A., Personal Communication, Rockton Research Center, Beloit Corp., Sept. 1989.

20. Mueller, T.J., "Flow Visualization by Direct Injection," In Fluid Mechanics Measurements, Chapter 7. (R. J.Goldstein, ed.) Hemisphere Publishing Corp., Washington, DC, 1985.

21. Peerhossaini, H., and Wesfreid, J.E., "Experimental Study of the Taylor-Görtler Instability," In Propagation in Systems Far from Equilibrium, Springer-Verlag, New York, 1988.

22. Pranckh, F. R., and Scriven, L. E., "The Physics of Blade Coating of Deformable Substrate," Coating Conference Proceedings, TAPPI Press, Atlanta, GA, 1988.

23. Quraishi, M.S., and Fahidy, T. Z., "Techniques for Flow Pattern Studies," Encyclopedia of Fluid Mechanics, Chapter 28. (N. P. Cheremisinoff, ed.) Gulf Publishing Co., Houston, TX, 1986.

24. Rautiainen, P. J., and Luomi, S. T., "High Speed Coating Processes - Trends and Developments," Coating Conference Proceedings, TAPPI Press, Atlanta, GA, 1984.

25. Ruckert, H., and Sommer, H. -P., "Development of a Coating Device for Low Coating Weight at High Production Speed and High Solids Content," *Wochbl. Papierfabrik.* **114**, 5, 1986.

26. Sollinger, H.-P., "Dynamic Coater -seine Auftrags- und Egalisiersysteme," *Wochbl. Papierfabrik.* **117**, 8, 1989.

27. Sommer, H. -P., "Applicating Systems for Coating Ultra-lightweight Coated and Machine Finish Pigmentized Papers," Coating Conference Proceedings, TAPPI Press, Atlanta, GA, 1988.

28. Swinney, H. L., and Di Prima, R. C., "Instabilities and Transition in Flow between Concentric Rotating Cylinders," In Hydrodynamic Instabilities and the Transition to Turbulence, (H.L. Swinney, J.P. Gollub, ed.) Springer-Verlag, New York, 1981.

29. Taylor, G.I., Stability of a Viscous Liquid Contained Between Two Rotating Cylinders. *Phil. Trans. Royal Soc. London*, Series A **223**, 289, 1923.

30. Triantafillopoulos, N. G., "Fluid Dynamics in Short Dwell Coater Ponds," Ph. D. Thesis (in progress), Institute of Paper Science and Technology, Atlanta, GA., 1990.

31. Triantafillopoulos, N.G., Farrington, T.E., "Flash X-ray Radiography Techniques for Visualizing Coating Flows," Coating Conference Proceedings, TAPPI Press, Atlanta, GA, 1988.

32. Triantafillopoulos, N.G., Rudemiller, G., Aidun, C., "Numerical Experiments of Short Dwell Coater Pond Flows, Int'l Symposium Pigment Coating Structure and Rheology," INSKO, Helsinki, Finland, Feb. 8-9, 1989.

33. Triantafillopoulos, N.G., Rudemiller, G., Farrington, T., Lindsay, J., "Numerical Simulation of Short Dwell Pond Flows. Engineering Conference Proceedings," TAPPI Press, Atlanta, GA, 1988.

34. Turai, L. L., "Analysis of the Blade Coating Process," *Tappi* **54**, 8, 1971.

35. Weigl, J., and Baumeister, M., "Influencing Factors and Their Effect on Coating Morphology," *Deut. Papierwirt* **3**, 147, 1980.

36. Wesfreid, J. E.; and Zaleski, S., Cellular Structures in Instabilities, Springer-Verlag, New York, 1984.